



Synthesis, Characterization, Thermal Decomposition And Antimicrobial Studies Of Iron (III) Complexes Of 2,3-(Diimino-4'-Antipyrinyl)Butane With Varying Counter Ions

BN Anila^{1,2*}, PK Radhakrishnan², MK Muraleedharan Nair³, Raisa Kabeer⁴ and VP Sylas⁴

¹Department of Chemistry, Government College Kottayam, Kerala, India

²School of Chemical Sciences, Mahatma Gandhi University, Kottayam, Kerala, India

³Department of Chemistry, Maharajas College, Ernakulam, Kerala India

⁴School of Environmental Sciences, Mahatma Gandhi University, Kottayam, Kerala, India

ABSTRACT

The synthesis, characterization, thermal decomposition and antimicrobial studies of the perchlorate, nitrate, thiocyanate, chloride and bromide complexes of iron(III) with 2,3-(diimino-4'-antipyrinyl) butane (BDAP) have been done. The characterization of the complexes were done by elemental analysis, molar conductance in non-aqueous solvents, IR and UV-Vis spectra and magnetic moment studies. The phenomenological, kinetic and mechanistic aspects of the complexes have been done by TG and DTG techniques. The kinetic parameters like activation energy, pre-exponential factor and entropy of activation were computed. The molar conductance and the infrared spectral studies reveal that one of the perchlorate ions is coordinated bidentately, two of the nitrate ions, thiocyanate ions, chloride ions and bromide ions are coordinated in a monodentate fashion. The UV-Vis spectral and magnetic moment data suggests a high spin octahedral geometry around the iron(III) ion in all the complexes. The mechanism for the thermal decomposition is random nucleation with one nucleus on each particle representing 'Mampel Model' for all the complexes except chloride complexes which has the mechanism phase boundary reaction representing spherical symmetry. Antimicrobial analyses of the ligand and the complexes reveal significantly higher activity for the metal complexes than the ligand against microorganisms. The structure activity relationship analysis of the complexes shows that, thiocyanate complexes have highest activity against bacteria and fungus.

Keywords: 2,3-(diimino-4'-antipyrinyl)butane; Antipyrine, iron(III) complexes; Thermogravimetry; Coats-Redfern Equation; Antimicrobial activity

INTRODUCTION

Metal complexes find interesting applications not only in the field of biology but also in various fields like medicine and catalysis [1-2]. Schiff base complexes derived from antipyrine have been extensively investigated and applied in the fields of biology and analytical, clinical and pharmacological areas [3]. Because of their different coordination possibilities with metal ions and consequently their flexible complexing behaviour, the synthesis and structural studies of pyrazole based ligands and their metal complexes has drawn the attention of many investigators [4-5]. In the present study we have synthesized five complexes of iron (III) with varying counter ions with the ligand 2,3-(diimino-4'-antipyrinyl)butane (BDAP). All the complexes were characterized using different analytical and spectral techniques. The phenomenological, kinetic and mechanistic aspects of the thermal analysis of the complexes were studied. The antimicrobial analyses of the complexes were also carried out.

EXPERIMENTAL SECTION

Materials

The metal salts used for the synthesis of complexes were purchased from E. Merck (AR grade), India Pvt. Ltd. The bromides, iodides and perchlorates of the metal were prepared from the metal carbonates (AR) and the respective acids by the following procedure. The metal carbonates were dissolved in 50% hot acids and the undissolved carbonate is removed by filtration. The filtrate was concentrated on a water bath to get the solid form of the salt. It was then dried under vacuum over phosphorous (V) oxide.

Ferric thiocyanate was prepared by the following method [6]. 30 ml of aqueous concentrated solution of $\text{FeCl}_3 \cdot 6\text{H}_2\text{O}$ and 70 ml of concentrated ammonium thiocyanate solutions were mixed in the ratio 1:3 by weight. The deep red ferric thiocyanate was formed and it was then extracted with diethyl ether. The ether layer containing the metal salt was separated by evaporation. All the salts were hygroscopic in nature and hence kept in a desiccator over a strong dehydrating agent.

Analyses of complexes

Iron present in the complexes were estimated gravimetrically. Chloride content was estimated by Volhard's method [7] and perchlorate content by Kurz's method [8]. The elemental analyses of the complexes were carried out using a Heraeus-CHN-Rapid Analyzer. Molar conductance of 10^{-3}M solutions of the complexes was measured using a Systronics conductivity bridge with a dip conductance cell having platinized platinum electrode. The infrared spectra was recorded in a Shimadzu FTIR 8400 S spectrophotometer in the range $4000\text{-}400\text{ cm}^{-1}$ using KBr pellet technique and in a Bruker IFS 66v FTIR spectrometer in the range $500\text{-}100\text{ cm}^{-1}$ using polyethylene powder. Electronic spectral studies of the Schiff base and the complexes in solid state were carried out on a Shimadzu UV-visible spectrometer UV-2450 in the range $190\text{-}1100\text{ nm}$. Magnetic susceptibility measurements were also done for the complexes.

Synthesis of the ligand 2,3-(diimino-4'-antipyrinyl) butane

The Schiff base ligand, 2,3-(diimino-4'-antipyrinyl) butane was prepared by the condensation between 2,3-butanedione and 4-aminoantipyrine in ethyl acetate medium for about 5 hours in 1:2 molar ratio. The yellow precipitate thus obtained was filtered and washed with hot ethyl acetate to remove the excess reactants. It was then recrystallized from ethanol and dried over phosphorous (V)oxide under vacuum. The yield was about 65%. The expected structure of the ligand is shown in figure 1. The purity of the ligand was checked by TLC, Infrared, mass, and NMR spectra and by elemental analysis. The melting point of the compound was found to be 245°C . The molecular formula and molecular weight of the ligand were $\text{C}_{26}\text{H}_{28}\text{N}_6\text{O}_2$ and 456.44 respectively. The elemental analysis data is as shown below; Found: C = 68.38 (68.41), H = 5.34 (6.18) N = 18.11 (18.40)

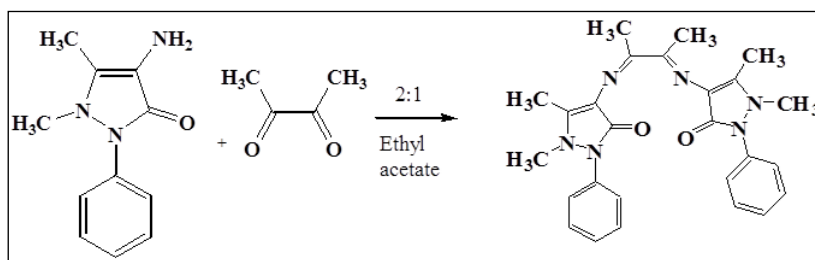


Figure 1: Scheme of synthesis of the ligand BDAP

Preparation of Iron (III) complexes

A quantity of 1 mmol of $\text{Fe}(\text{ClO}_4)_3 \cdot 6\text{H}_2\text{O}$, $\text{Fe}(\text{NO}_3)_3 \cdot 6\text{H}_2\text{O}$, $\text{FeBr}_3 \cdot 6\text{H}_2\text{O}$ or $\text{Fe}(\text{SCN})_3 \cdot 6\text{H}_2\text{O}$, in methanol (10mL) or $\text{FeCl}_3 \cdot 6\text{H}_2\text{O}$ in acetone (10mL) was added to a boiling suspension of 1.2mmol of BDAP in ethyl acetate (100mL). The mixture was refluxed for about 5 hours on a steam bath. The precipitated complexes formed were filtered and washed repeatedly with hot ethyl acetate to remove the excess ligand and were recrystallized from ethanol. It was then dried over phosphorous (V) oxide under vacuum.

RESULTS AND DISCUSSION

The iron(III) complexes are dark brown non-hygroscopic solids except the thiocyanate complex which is reddish brown in colour. These are soluble in acetonitrile, benzene, DMF, DMSO, ethanol and methanol and are insoluble in acetone, ethyl acetate and nitrobenzene.

Elemental analysis

The metal, bromide, chloride, perchlorate, carbon, nitrogen and hydrogen content in the iron(III) complexes were determined and presented in table 1. The data suggests that the complexes may be formulated as $\text{Fe}(\text{BDAP})\text{X}_3$ where $\text{X} = \text{ClO}_4^-$, NO_3^- , SCN^- , Cl^- or Br^- .

Table 1: Analytical data^a of the Iron (III) complexes of BDAP a: calculated values in parentheses

| Complex/Molecular formula/ Formula weight | Metal (%) | Anion (%) | Carbon (%) | Hydrogen (%) | Nitrogen (%) | Melting point °C |
|---|-----------|-----------|------------|--------------|--------------|------------------|
| $[\text{Fe}(\text{BDAP})(\text{ClO}_4)](\text{ClO}_4)_2$ | 6.71 | 36.74 | 38.42 | 3.41 | 10.22 | 178 |
| $\text{C}_{26}\text{Cl}_3\text{FeH}_{28}\text{N}_6\text{O}_{12}$ (810.64) | -6.88 | -36.8 | -38.49 | -3.45 | -10.36 | |
| $[\text{Fe}(\text{BDAP})(\text{NO}_3)_2]\text{NO}_3$ | 8.06 | - | 44.82 | 4.21 | 18.11 | 165 |
| $\text{C}_{26}\text{FeH}_{28}\text{N}_9\text{O}_9$ (698.28) | -7.99 | | -44.72 | -4 | -18.04 | |
| $[\text{Fe}(\text{BDAP})(\text{SCN})_2]\text{SCN}$ | 8.18 | - | 50.65 | 4 | 18.29 | 160 |
| $\text{C}_{29}\text{FeH}_{28}\text{N}_9\text{S}_3$ (686.28) | -8.13 | | -50.7 | -4.07 | -18.35 | |
| $[\text{Fe}(\text{BDAP})\text{Cl}_2]\text{Cl}$ | 9.1 | 17.52 | 50.32 | 4.64 | 13.42 | 172 |
| $\text{C}_{26}\text{Cl}_3\text{FeH}_{28}\text{N}_6$ (618.64) | -9.03 | -17.2 | -50.47 | -4.52 | -13.57 | |
| $[\text{Fe}(\text{BDAP})\text{Br}_2]\text{Br}$ | 7.54 | 31.62 | 40.99 | 3.65 | 11.14 | 168 |
| $\text{Br}_2\text{C}_{26}\text{FeH}_{28}\text{N}_6$ (752.00) | -7.42 | -31.87 | -41.48 | -3.72 | -11.16 | |

Electrical conductance

The molar conductance values of the iron (III) complexes of BDAP (10^{-3}M solution) were measured in acetonitrile, DMF, ethanol and methanol and the values are given in table 2. The molar conductance values fall in the range suggests 1:2 electrolytes for perchlorate complex and 1:1 for nitrate, thiocyanate, chloride and bromide complexes [9]. Thus the complexes may be formulated as $[\text{Fe}(\text{BDAP})\text{X}]\text{X}_2$ ($\text{X} = \text{ClO}_4^-$) and $[\text{Fe}(\text{BDAP})\text{X}_2]\text{X}$ ($\text{X} = \text{NO}_3^-$, SCN^- , Cl^- or Br^-).

Table 2: Molar Conductance^a data of the Iron (III) Complexes^b of BDAP ^a $\text{ohm}^{-1}\text{cm}^2\text{mol}^{-1}$ ^b 10^{-3}M solution

| Complex | Molar conductance | | | | Type of electrolyte |
|--|-------------------|-------|----------|---------|---------------------|
| | Acetonitrile | DMF | Methanol | Ethanol | |
| $[\text{Fe}(\text{BDAP})(\text{ClO}_4)](\text{ClO}_4)_2$ | 285.9 | 155.6 | 178.4 | 75.02 | 01:02 |
| $[\text{Fe}(\text{BDAP})(\text{NO}_3)_2]\text{NO}_3$ | 167.45 | 84.41 | 108.57 | 61.72 | 01:01 |
| $[\text{Fe}(\text{BDAP})(\text{SCN})_2]\text{SCN}$ | 132.52 | 71.26 | 105.2 | 59.42 | 01:01 |
| $[\text{Fe}(\text{BDAP})\text{Cl}_2]\text{Cl}$ | 122.4 | 68.02 | 95.14 | 69.07 | 01:01 |
| $[\text{Fe}(\text{BDAP})\text{Br}_2]\text{Br}$ | 121.3 | 93.54 | 100.15 | 52.65 | 01:01 |

Infrared spectra

The important infrared spectral bands of BDAP and its iron(III) complexes together with the tentative assignments are given in Table 3.

The infrared spectrum of the ligand BDAP shows strong bands at 1649 and 1593cm^{-1} , characteristic of both carbonyl [10] and azomethine [11-12] groups respectively. The band at 1649cm^{-1} , characteristic of carbonyl groups in BDAP is found to be shifted to the region 1637 - 1625cm^{-1} in all the complexes showing that both the carbonyl oxygens are coordinated in these complexes [13]. Also the intense band due to azomethine nitrogen is shifted to the region 1587 - 1566cm^{-1} all the complexes indicating the coordination of both the azomethine nitrogens [14].

From the infrared spectral data it is concluded that the Schiff base BDAP acts as a neutral tetradentate ligand, coordinating through both the carbonyl oxygens and both the azomethine nitrogens resulting in the formation of three five membered rings, thereby imparting considerable stability to the complexes.

In the perchlorate complex, the triply split band maxima observed at 1143 , 1116 and 1018cm^{-1} are due to ν_8 , ν_6 and ν_1 vibrations respectively of the perchlorate ion of C_{2v} symmetry indicating the coordination of perchlorate ion in a bidentate fashion [15]. But the band observed at 1080cm^{-1} is assigned to the ν_3 vibration of uncoordinated perchlorate ion of T_d symmetry [16]. Thus indicate the presence of both the uncoordinated and bidentately coordinated perchlorate ion. The vibrational frequencies corresponding to ν_2 and ν_3 vibrations of the perchlorate (C_{2v}) ion is observed at 932 and 642cm^{-1} respectively and ν_4 vibration of the perchlorate (T_d) ion is observed at 624cm^{-1} , also support the coexistence of both uncoordinated and bidentately coordinated perchlorate ion in the complex [15].

In the nitrate complex, two medium bands at 1477 and 1312cm^{-1} are observed which are attributable to the ν_4 and ν_1 stretching vibrations respectively of the nitrate ion of C_{2v} symmetry [17]. Since the difference between ν_4 and ν_1 is 165cm^{-1} , the nitrate ion is monodentately coordinated [18]. A very strong band observed at 1382cm^{-1} indicates the presence of uncoordinated nitrate ion in this complex which is due to ν_3 vibration of the nitrate ion of D_{3h} symmetry [19]. This is

supported by another medium intensity band observed at 825 cm^{-1} which is attributed to the ν_2 vibration of the uncoordinated nitrate ion of D_{3h} symmetry.

In the thiocyanate complex a sharp band observed at 2054 cm^{-1} is attributed to N coordinated thiocyanate ion [20]. Further the presence of bands at 853 and 480 cm^{-1} stands as an additional evidence for the presence of N coordinated thiocyanate ion in the complex.

In the far IR spectrum of the chloro and bromo complexes the Fe-Br and Fe-Cl bands are observed at 280 and 279 cm^{-1} respectively which are not present in the spectrum of the ligand.

The above IR spectral results are in conformity with the conductance data that one of the perchlorates as well as two of the nitrates, thiocyanates, chlorides and bromides is coordinated to the metal ion in these complexes. Further the $\nu_{\text{Fe-O}}$ and $\nu_{\text{Fe-N}}$ stretching vibrations are observed at about 552 cm^{-1} and 456 cm^{-1} respectively in all the complexes [21].

Table 3: Important infrared spectral bands (cm^{-1}) of BDAP and its Iron (III) complexes

| BDAP | [Fe(BDAP)(ClO ₄)](ClO ₄) ₂ | [Fe(BDAP)(NO ₃) ₂]NO ₃ | [Fe(BDAP)(SCN) ₂]SCN | [Fe(BDAP)Cl ₂]Cl | [Fe(BDAP)Br ₂]Br | Assignments |
|------|---|---|----------------------------------|------------------------------|------------------------------|--|
| 1649 | 1625 | 1629 | 1629 | 1629 | 1637 | $\nu_{\text{C=O}}$ |
| 1593 | 1570 | 1556 | 1564 | 1575 | 1564 | $\nu_{\text{C=N}}$ |
| | 1143 | | | | | ν 8coordinated ClO ₄ |
| | 1116 | | | | | ν 6coordinated ClO ₄ |
| | 1018 | | | | | ν 1coordinated ClO ₄ |
| | 932 | | | | | ν 2coordinated ClO ₄ |
| | 636 | | | | | ν 3coordinated ClO ₄ |
| | 1080 | | | | | ν 3uncoordinated ClO ₄ |
| | 624 | | | | | ν 4 uncoordinated ClO ₄ |
| | | 1477 | | | | ν 4coordinated NO ₃ |
| | | 1312 | | | | ν 1coordinated NO ₃ |
| | | | | | | ν 2coordinated NO ₃ |
| | | 1382 | | | | ν 3uncoordinated NO ₃ |
| | | 825 | | | | ν 2uncoordinated NO ₃ |
| | | | 2054 | | | $\nu_{\text{C-N}}$ |
| | | | 853 | | | $\nu_{\text{C-S}}$ |
| | | | 480 | | | ν_{NCS} |
| | 279 | | | 279 | 280 | $\nu_{\text{Fe-Cl/Br}}$ |
| | 552 | 554 | 553 | 554 | 556 | $\nu_{\text{Fe-O}}$ |
| | 452 | 453 | 452 | 454 | 453 | $\nu_{\text{Fe-N}}$ |

Electronic spectral studies and magnetism

The electronic spectral bands of the complexes of BDAP with tentative assignments are listed in table 4. The electronic spectra of the ligand BDAP shows two absorption maxima at 26810 and 42735 cm^{-1} corresponding to $n \rightarrow \pi^*$ and $\pi \rightarrow \pi^*$ transitions respectively [21]. But in Iron(III) complexes, compared to BDAP $n \rightarrow \pi^*$ transitions are found to be blue shifted to the regions 27933 - 29499 cm^{-1} and the $\pi \rightarrow \pi^*$ transitions are found to be red shifted to 36630 - 40983 cm^{-1} [22]. The absorption band observed in the region 20040 - 22371 cm^{-1} of the complexes may be assigned to ${}^6A_{1g} \rightarrow {}^4T_{1g}$ transition which is in agreement with octahedral geometry around the iron(III) ion [23]. Also an intense band observed in the region 32786 - 34246 cm^{-1} in all the complexes may be due to charge transfer transition.

The observed magnetic moment values of all the complexes are in the range 4.9 - 5.96 BM suggest a high spin octahedral geometry around Fe (III) in all these complexes [24-25]. In high spin octahedral iron (III) complexes the expected value is 5.9 BM . The lower values observed for perchlorate, nitrate and chloride complexes indicate metal-metal interaction [26].

Thermogravimetric analyses

The phenomenological, mechanistic as well as kinetic aspects of thermal decomposition of iron(III) complexes of BDAP were done and the data are presented in tables 5 to 7.

Phenomenological Aspects

All the iron (III) complexes undergo a two stage decomposition pattern except perchlorate complex, which undergoes charring at 214°C due to thermal instability to withstand temperature higher than 214°C [27].

In nitrate complex there is no mass loss up to 191°C indicating the absence of water or any solvent molecules. The first stage starts at 191°C and ends at 356°C . The corresponding mass loss (26.49%) is due to the decomposition of three nitrate ions. The maximum rate of mass loss occurs at 256°C as indicated by DTG peak. The second stage starts at 356°C and ends at 420°C with a DTG peak at 390°C . The corresponding mass loss (65.46%) is due to the

decomposition of the BDAP molecule. The decomposition gets completed at 420°C and the final residue is qualitatively proved to be anhydrous FeO.

In thiocyanate complex there is no mass loss up to 179°C indicating the absence of water or any solvent molecules. The first stage starts at 179°C and ends at 373°C. The corresponding mass loss (24.64%) is due to the decomposition of three thiocyanate ions. The maximum rate of mass loss occurs at 235°C as indicated by DTG peak. The second stage starts at 373°C and ends at 588°C with a DTG peak at 3543°C. The corresponding mass loss (65.27%) is due to the decomposition of the BDAP molecule. The decomposition gets completed at 588°C and the final residue is qualitatively proved to be anhydrous FeO.

In chloro complex there is no mass loss up to 181°C indicating the absence of water or any solvent molecules. The first stage starts at 181°C and ends at 317°C. The corresponding mass loss (17.56%) is due to the decomposition of three chloride ions. The maximum rate of mass loss occurs at 254°C as indicated by DTG peak. The second stage starts at 317°C and ends at 572°C with a DTG peak at 445°C. The corresponding mass loss (73.24%) is due to the decomposition of the BDAP molecule. The decomposition gets completed at 572°C and the final residue is qualitatively proved to be anhydrous FeO.

In bromo complex there is no mass loss up to 202°C indicating the absence of water or any solvent molecules. The first stage starts at 202°C and ends at 363°C. The corresponding mass loss (60.54%) is due to the decomposition of one molecule of BDAP. The maximum rate of mass loss occurs at 328°C as indicated by DTG peak. The second stage starts at 363°C and ends at 648°C with a DTG peak at 445°C. The corresponding mass loss (31.69%) is due to the decomposition of three bromide ions. The decomposition gets completed at 648°C and the final residue is qualitatively proved to be anhydrous FeO.

From the above results we can conclude that all the complexes except perchlorate complex undergoes two stage decomposition and the mass loss found is in good agreement with the calculated values with a final product FeO. The perchlorate complex which is the least stable complex undergoes charring. The thermal stability of the complexes is in the order bromide > thiocyanate > chloride > nitrate > perchlorate.

Table 4: Electronic Spectral data and magnetic moment values of Iron (III) complexes of BDAP

| Complex | Abs. Maxima (cm ⁻¹) | Tentative Assignments | μ_{eff} (BM) |
|---|---------------------------------|---|-------------------------|
| BDAP | 26,810 | n- π^* | |
| | 42,735 | $\pi-\pi^*$ | |
| [Fe(BDAP)(ClO ₄) ₂](ClO ₄) ₂ | 29449 | n- π^* | 4.99 |
| | 39682 | $\pi-\pi^*$ | |
| | 34129 | Charge Transfer | |
| | 20,790 | ⁶ A _{1g} → ⁴ T _{1g} | |
| | 27,933 | n- π^* | |
| [Fe(BDAP)(NO ₃) ₂] ₂ NO ₃ | 36630 | $\pi-\pi^*$ | 5.68 |
| | 33557 | Charge Transfer | |
| | 22371 | ⁶ A _{1g} → ⁴ T _{1g} | |
| | 28653 | n- π^* | |
| [Fe(BDAP)(SCN) ₂] ₂ SCN | 39682 | $\pi-\pi^*$ | 5.95 |
| | 34246 | Charge Transfer | |
| | 20833 | ⁶ A _{1g} → ⁴ T _{1g} | |
| | 28,571 | n- π^* | |
| | 40983 | $\pi-\pi^*$ | |
| [Fe(BDAP)Cl ₂] ₂ Cl | 33783 | Charge Transfer | 5.55 |
| | 20040 | ⁶ A _{1g} → ⁴ T _{1g} | |
| | 29,240 | n- π^* | |
| | 38167 | $\pi-\pi^*$ | |
| [Fe(BDAP)Br ₂] ₂ Br | 32786 | Charge Transfer | 5.96 |
| | 21,552 | ⁶ A _{1g} → ⁴ T _{1g} | |

Kinetic aspects

The activation energies (E) of all the complexes of different stages of thermal decomposition are in the range 31.24 to 158.36 KJmol⁻¹ and the corresponding values of pre-exponential factor for these complexes vary in the range 3.62× 10⁻² to 841.55 S⁻¹. The respective values of entropy of activation (ΔS) are in the range -196.29 to -278.88Jmol⁻¹. It is observed that the energy of activation and pre-exponential factor of the second stage of decomposition of all the complexes except nitrate and thiocyanate complexes are lower than that of the first stage. But the entropy of activation of the second stage of decomposition of all the complexes except chloride and bromide complexes are higher than that of the first stage. The negative values of entropy of activation indicate that the activated complex has a more ordered structure than the reactant and the reactions are slower than the normal [28].

Mechanistic aspects

The highest values of the magnitude of correlation coefficient is obtained for the equation $g(\alpha) = -\ln(1-\alpha)$ for all the stages of decomposition of all the complexes except chloride complex. Hence the mechanism for the decomposition is random nucleation with one nucleus on each particle representing 'Mampel Model' [29].

For the first stage of chloride complex, the highest value of the magnitude of correlation coefficient is obtained for the equation $g(\alpha) = 1-(1-\alpha)^{1/3}$. Hence the mechanism is phase boundary reaction representing spherical symmetry.

Table 5: Phenomenological data for the thermal decomposition of the Iron (III) complexes of BDAP

| Complexes | Stages of Decomposition | Temp. (°C) | DTA peak (°C) | Residual species | Decomposition species | Total Mass Loss (%) | |
|---|-------------------------|------------|---------------|------------------|----------------------------|---------------------|------------|
| | | | | | | Found | Calculated |
| [Fe(BDAP)(ClO ₄) ₂](ClO ₄) ₂ | I | 185-214 | 196 | Nil | charring of the whole mass | 98 | 100 |
| [Fe(BDAP)(NO ₃) ₂](NO ₃) | I | 191-356 | 256 | FeO | Three nitrate ions | 26.49 | 26.63 |
| | II | 356-420 | 390 | | One molecule BDAP | 65.46 | 65.37 |
| [Fe(BDAP)(SCN) ₂](SCN) | I | 179-373 | 235 | FeO | Three thiocyanate ions | 24.64 | 25.35 |
| | II | 373-588 | 543 | | One molecule BDAP | 65.27 | 66.5 |
| [Fe(BDAP)Cl ₂](Cl) | I | 180-317 | 254 | FeO | Three chloride ions | 17.56 | 17.19 |
| | II | 317-572 | 445 | | one molecule of BDAP | 73.24 | 73.78 |
| [Fe(BDAP)Br ₂](Br) | I | 202-363 | 328 | FeO | one molecule of BDAP | 60.54 | 60.6 |
| | II | 363-648 | 445 | | Three bromide ions | 31.69 | 31.87 |

Table 6: Kinetic parameters for the thermal decomposition of the Iron(III) complexes of BDAP

| Complex | Stages of Decomposition | E (KJmol ⁻¹) | A (s ⁻¹) | ΔS (JK ⁻¹ mol ⁻¹) |
|--|-------------------------|--------------------------|----------------------|--|
| [Fe(BDAP)(NO ₃) ₂](NO ₃) | I | 84.59 | 36.95 | -219.56 |
| | II | 61.57 | 0.3609 | -260.26 |
| [Fe(BDAP)(SCN) ₂](SCN) | I | 64.97 | 1.2126 | -248.66 |
| | II | 61.69 | 0.1726 | -268.62 |
| [Fe(BDAP)Br ₂](Br) | I | 58.37 | 0.7342 | -252.93 |
| | II | 100.67 | 2.155 | -247.71 |
| [Fe(BDAP)Cl ₂](Cl) | I | 31.24 | 3.62 | -278.88 |
| | II | 158.36 | 841.55 | -196.29 |

Table 7: Correlation coefficients calculated using the nine forms of g(α) for Iron(III) complexes of BDAP

| No | Forms of g(α) | Correlation coefficient (r) | | | | | | | |
|----|----------------------------------|-----------------------------|----------|---------------------|----------|------------------|----------|-----------------|----------|
| | | Nitrate complex | | Thiocyanate complex | | Chloride complex | | Bromide complex | |
| | | Stage I | Stage II | Stage I | Stage II | Stage I | Stage II | Stage I | Stage II |
| 1 | α^2 | -0.9448 | -0.9889 | -0.9671 | -0.9612 | -0.9735 | -0.9616 | -0.9819 | -0.9516 |
| 2 | $\alpha+(1-\alpha)\ln(1-\alpha)$ | -0.9683 | -0.9922 | -0.9845 | -0.9723 | -0.9806 | -0.9669 | -0.9889 | -0.9594 |
| 3 | $[1-(1-\alpha)^{1/3}]^2$ | -0.9137 | -0.9817 | -0.9457 | -0.9217 | -0.9583 | -0.9472 | -0.951 | -0.9423 |
| 4 | $[(1-2/3\alpha)]-1-\alpha^{2/3}$ | -0.9783 | -0.9933 | -0.9939 | -0.9763 | -0.9831 | -0.9688 | -0.9912 | -0.9622 |
| 5 | $-\ln(1-\alpha)$ | -0.9927 | -0.9957 | -0.9711 | -0.987 | -0.9905 | -0.9735 | -0.9963 | -0.9723 |
| 6 | $[-\ln(1-\alpha)]^{1/2}$ | -0.991 | -0.9932 | -0.9652 | -0.9775 | -0.9859 | -0.9641 | -0.9907 | -0.9674 |
| 7 | $[-\ln(1-\alpha)]^{1/3}$ | -0.9885 | -0.9876 | -0.9571 | -0.9548 | -0.9776 | -0.9497 | -0.9671 | -0.9616 |
| 8 | $1-(1-\alpha)^{1/2}$ | -0.9802 | -0.9921 | -0.993 | -0.9713 | -0.9811 | -0.965 | -0.9882 | -0.9607 |
| 9 | $1-(1-\alpha)^{1/3}$ | -0.9892 | -0.9936 | -0.9947 | -0.9775 | -0.9847 | -0.968 | -0.9918 | -0.9647 |

Antimicrobial studies

The antibacterial and antifungal results of Fe (III) complexes are summarized in Table 8 and 9. All the complexes were showing a very good antibacterial and antifungal activity against all the six gram positive and gram negative bacteria and the fungus compared to the standard. Generally, the complexes have higher activity than the Schiff base ligand. A

possible explanation for the observed increased activity upon chelation is that the positive charge of the metal in chelated complex is partially shared with the ligand's donor atoms so that there is an electron delocalization over the whole chelate ring. This, in turn, will increase the lipophilic character of the metal [30]. The graphical representation of their activity against bacteria and fungus are shown in Figure 2 and 3. From the figure we can see that $[\text{Fe}(\text{BDAP})(\text{SCN})_2]\text{SCN}$ complex is showing higher activity against bacteria and fungus compared to other complexes and ligand.

Table 8: Antibacterial activity of BDAP and its Iron (III) Complexes (Zone diameter in mm)

| Compound | <i>V.parahaemolyticus</i> | <i>S.typhi</i> | <i>A. hydrophila</i> | <i>B. subtilis</i> | <i>E.coli</i> | <i>S.weltevreden</i> |
|--|---------------------------|----------------|----------------------|--------------------|---------------|----------------------|
| BDAP | 0 | 20 | 23 | 0 | 19 | 19 |
| $[\text{Fe}(\text{BDAP})(\text{ClO}_4)](\text{ClO}_4)_2$ | 16 | 23 | 22 | 13 | 20 | 21 |
| $[\text{Fe}(\text{BDAP})(\text{NO}_3)_2]\text{NO}_3$ | 16 | 22 | 25 | 12 | 20 | 20 |
| $[\text{Fe}(\text{BDAP})(\text{SCN})_2]\text{SCN}$ | 13 | 26 | 28 | 17 | 24 | 24 |
| $[\text{Fe}(\text{BDAP})\text{Cl}_2]\text{Cl}$ | 17 | 23 | 22 | 13 | 20 | 21 |
| $[\text{Fe}(\text{BDAP})\text{Br}_2]\text{Br}$ | 19 | 22 | 24 | 14 | 21 | 21 |
| Standard (Streptomycin) | 4 | 15 | 16 | 13 | 12 | 15 |

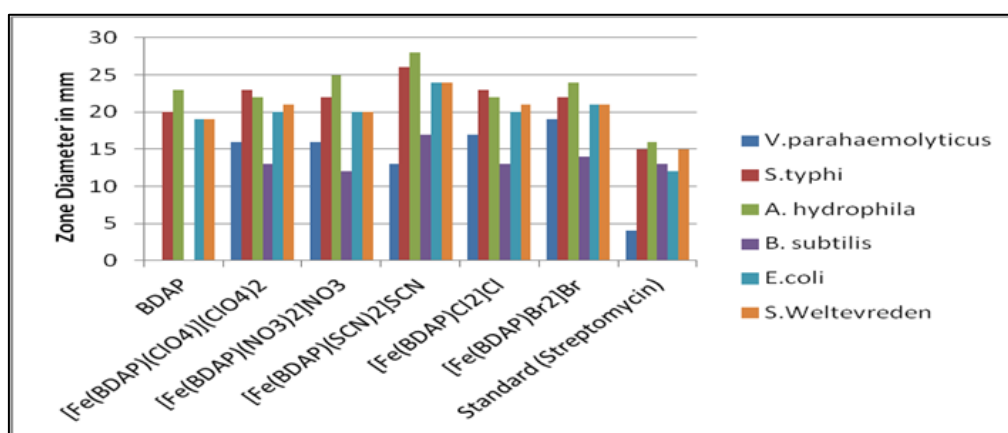


Figure 2: Graphical representation of Antibacterial Analyses of BDAP and its Fe (III) complexes

Table 8: Antifungal activity of BDAP and its Iron (III) Complexes (Zone diameter in mm)

| Compound | <i>Trichophyton tonsurans</i> (Zone diameter in mm) |
|--|--|
| BDAP | 14 |
| $[\text{Fe}(\text{BDAP})(\text{ClO}_4)](\text{ClO}_4)_2$ | 16 |
| $[\text{Fe}(\text{BDAP})(\text{NO}_3)_2]\text{NO}_3$ | 17 |
| $[\text{Fe}(\text{BDAP})(\text{SCN})_2]\text{SCN}$ | 18 |
| $[\text{Fe}(\text{BDAP})\text{Cl}_2]\text{Cl}$ | 17 |
| $[\text{Fe}(\text{BDAP})\text{Br}_2]\text{Br}$ | 17 |
| Chlorothalonil | 34 |
| DMSO | 0 |

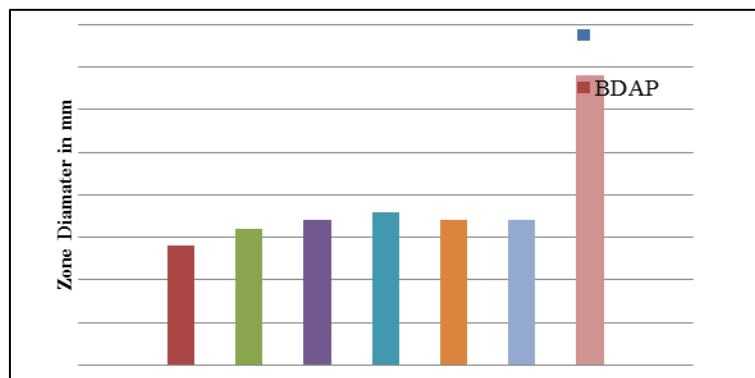


Figure 3: Graphical representation of Antifungal Analyses of BDAP and its Fe(III) complexes

CONCLUSION

According to the elemental analyses and molar conductance data, the iron (III) complexes of BDAP may be formulated as $[\text{Fe}(\text{BDAP})\text{ClO}_4](\text{ClO}_4)_2$ and $[\text{Fe}(\text{BDAP})\text{X}]\text{X}$ (where $\text{X} = \text{NO}_3^-$, SCN^- , Cl^- or Br^-). The infrared spectral data suggest that BDAP acts as a neutral tetradentate ligand coordinating through both the carbonyl oxygens and azomethine nitrogens. The molar conductance and the infrared spectral studies reveal that one of the perchlorate ions is coordinated bidentately, two of the nitrate ions are coordinated in a monodentate fashion and two of the thiocyanate ions are coordinated monodentately through the nitrogen atom. In the case of halide complexes, two of the chlorides and two of the bromides are coordinated. The electronic spectra and magnetic moment suggest high spin octahedral geometry around the iron (III) ion in all the complexes. The thermogravimetric analyses also confirmed the above observations. The antibacterial and antifungal studies show that all the complexes exhibit a very good activity against some selective pathogenic bacteria and fungus. Based on the results of the present study, the tentative structures of the complexes are shown in Figure 4.

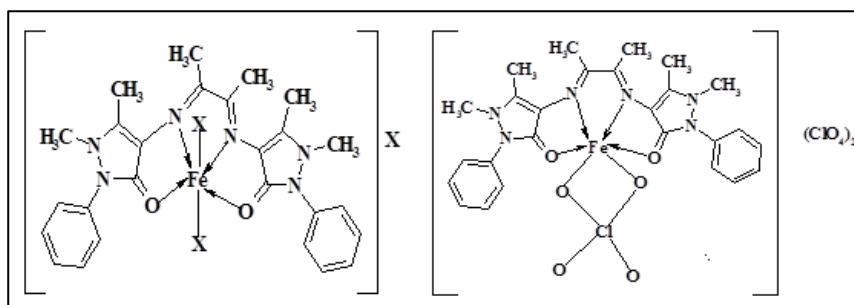


Figure 4: Tentative structures of iron(III) complexes of BDAP. (where $\text{X} = \text{NO}_3^-$, SCN^- , Cl^- or Br^-)

ACKNOWLEDGEMENT

The authors are indebted to Mahatma Gandhi University, Kottayam, Kerala, India, for providing the laboratory facilities. The author ABN is thankful to UGC for providing RGNF fellowship.

REFERENCES

- [1] G Turan-Zitounia; M Sivacia; FS Kilic; K Erol, *Eur. J. Med. Chem.*, **2001**, 36(7-8), 685-689.
- [2] NV Bashkatova; EI Korotkova; YA Karbaino; AY Yagovkin; AA Bakibaev, *J. Pharm. Biomed. Anal.*, **2005**, 37, 1143-1147.
- [3] C Maurya; A Pandey; J Chaurasia; H Martin, *J. Mol. Struct.*, **2006**, 798(1-3), 89-101.
- [4] RJ Fessenden, JS Fessenden. *Organic Chemistry*. 6th Edition, Brooks/Cole Publishing Company, USA, **1998**.
- [5] AH Brundic; B Kaitner; B Kamenar; VM Leovac; EZ Iveges; N Juranic, *Inorg. Chim. Acta*, **1991**, 188, 151-158.
- [6] ANS Ram; S Sarasukutty; CP Prabhakaran, *Curr.Sci.*, **1976**, 45, 514-516.
- [7] AI Vogel. *A Text Book of Quantitative Inorganic Analysis*. 3rd Edition, ELBS, London, 1961.
- [8] E Kurz; G Kober; M Berl, *Anal. Chem.*, **1958**, 30,1983.
- [9] WJ Geary. *Coord. Chem. Rev.*, **1971**, 7, 81.
- [10] S Joseph; PK Radhakrishnan. *Synth. React. Inorg. Met-Org. Chem.*,**1998**, 28(3), 423-435.
- [11] H Md. Tofazzal; N Tarafdal; Saravanan; A K Crouse, *Trans.Met.Chem.*, **2001**, 26(6), 613-618.
- [12] KC Raju; NT Madhu; PK Radhakrishnan, *Synth. React. Inorg. Met.-Org.Chem.*, **2002**, 32(6), 1115-1125.
- [13] KP Deepa; KK Aravindakshan, *Synth. React. Inorg. Met. Org. Chem.*, **2000**, 30(8), 1601-1616.
- [14] M Salehi; F Rahimifar; M Kubicki; A. Asadi, *Inorganica Chimica Acta*. 2016, 443, 28-35.
- [15] NT Madhu; PK Radhakrishnan, *Synth.React. Inorg. Met-Org. Nano-Met. Chem.*, **2001**, 31(9), 1663-1673.
- [16] RC Mayura; DD Mishra; PK Trivedi; A Gupta, *Synth.React. Inorg. Met-Org. Nano-Met. Chem.*, 1994, 24 (1), 17-28.
- [17] NT Madhu; PK Radhakrishnan, *Trans.Met. Chem.*, **2000**, 25, 287-292.
- [18] B Kuncheria; G Devi; P Indrasenan, *Inorganica Chimica Acta.*, **1989**, 155, 255-258.
- [19] K Das; TN Mandal; S Roy; S Gupta; AK Barik; P Mitra; AL Rheingold; SK Kar, *Polyhedron*, 2010, 29(15), 2892-2899.
- [20] BS Garg; DN Kumar, *Spectrochim. Acta*, **2003**, 59A, 229-234.
- [21] G Wang; JC Chang, *Synth. React. Inorg. Met-Org. Chem.*, **1986**, 16, 1121-1133.
- [22] PM Vimal Kumar; PK Radhakrishnan, *Inorg. Chim. Acta*, **2011**, 375, 84-92.

-
- [23] BN Ghose; KM Lasisi, *Synth. React. Inorg. Met-Org. Chem.*, **1986**, 16, 1189-1196.
- [24] N Mondal; DK Dey; S Mitra; KM Abdulmalik, *Polyhedron*, **2000**, 19, 2707-2711.
- [25] EC Okafor; BA Uzoukwu, *Synth. React. Inorg. Met. – Org. Nano-Met. Chem.*, **1992**, 22 (7), 921-927.
- [26] M del C Fernandez; RB de la Calle; A Macias; LV Matarranz; PP Lourida, *Polyhedron*, **2008**, 27(16), 3391-3197.
- [27] WW Wendlandt. *Thermal Analysis*, Third Edition, John Wiley & Sons, New York, 1986.
- [28] Suresh Mathew; CGR. Nair; KN Nainan, *Thermochimica Acta*, **1989**, 144(1), 33-43.
- [29] V Indira; G Parameswaran, *J. Therm. Anal.*, **1993**, 39, 1417.
- [30] S Chandra; A Kumar. *Spectrochim. Acta*. **2007**, 68A, 1410-1415.